Molecular Cloning of the Heparin/Heparan Sulfate Δ4,5 Unsaturated Glycuronidase from *Flavobacterium heparinum*, Its Recombinant Expression in *Escherichia coli*, and Biochemical Determination of Its Unique Substrate Specificity†

James R. Myette,‡ Zachary Shriver,‡ Tanyel Kiziltepe,§ Maitland W. McLean,||,⊥ Ganesh Venkataraman,# and Ram Sasisekharan*,‡

Division of Biological Engineering, Department of Chemistry, and Division of Health Sciences and Technology, Massachusetts Institute of Technology, 77 Massachusetts Avenue, Cambridge, Massachusetts 02139, and Department of Molecular and Cell Biology, University of Aberdeen, Marischal College, United Kingdom

Received December 11, 2001; Revised Manuscript Received March 13, 2002

ABSTRACT: The soil bacterium *Flavobacterium heparinum* produces several enzymes that degrade heparan sulfate glycosaminoglycans (HSGAGs) in a sequence-specific manner. Among others, these enzymes include the heparinases and an unusual glycuronidase that hydrolyzes the unsaturated Δ4,5 uronic acid at the nonreducing end of oligosaccharides resulting from prior heparinase eliminative cleavage. We report here the molecular cloning of the Δ4,5 glycuronidase gene from the flavobacterial genome and its recombinant expression in *Escherichia coli* as a highly active enzyme. We also report the biochemical and kinetic characterization of this enzyme, including an analysis of its substrate specificity. We find that the Δ4,5 glycuronidase discriminates on the basis of both the glycosidic linkage and the sulfation pattern within its saccharide substrate. In particular, we find that the glycuronidase displays a strong preference for 1→4 linkages, making this enzyme specific to heparin/heparan sulfate rather than 1→3 linked glycosaminoglycans such as chondroitin/dermatan sulfate or hyaluronan. Finally, we demonstrate the utility of this enzyme in the sequencing of heparinase-derived HSGAG oligosaccharides.

Glycosaminoglycans (GAGs) are linear, acidic polysaccharides that exist ubiquitously in nature as residents of the extracellular matrix and at the cell surface of many different organisms (*1*). In addition to a structural role, GAGs act as critical modulators of a number of biochemical signaling events (*2*) requisite for cell growth and differentiation, cell adhesion and migration, and tissue morphogenesis. The heparan sulfate glycosaminoglycans (HSGAGs)[1] are a particular class of GAGs that have emerged as key players in many different biological processes ranging from angiogenesis (*3*) and cancer biology (*4*) to microbial pathogenesis (*5*). HSGAGs have also recently been shown to play a fundamental role in multiple aspects of development (*6*).

HSGAGs are able to mediate these different biological events as a consequence of their considerable structural diversity (*7*, *8*). This chemical heterogeneity is due largely to the differential sulfation pattern present for each disaccharide unit within the oligosaccharide chain. Adding to this structural variability is the C5 epimerization of the uronic acid that occurs at select chain positions. Taken together, these structural determinants impart a unique sequence to each HSGAG chain. In turn, this sequence dictates a critical HSGAG−protein interaction (*9*).

A determination of GAG sequence, however, has been technically challenging. To begin with, these polysaccharides are naturally present in very limited quantities, which, unlike other biopolymers such as proteins and nucleic acids, cannot be readily amplified. Second, due to their highly charged character and structural heterogeneity, HSGAGs are not easily isolated from biological sources in a highly purified state. Compounding this reality has historically been the lack of sequence-specific tools to cleave these linear polysaccharide chains in a manner analogous to DNA sequencing or restriction mapping. Recent chemical and enzymatic approaches have been used to cleave GAGs in a sequence-specific fashion. These HSGAG degradation procedures have been used in conjunction with several analytical methods such as gel electrophoresis (*10*, *11*), HPLC, and mass spectroscopy (*12*) to sequence the polysaccharides. We have refined this GAG sequencing approach by using tandem

† This work was supported in part by NIH Grants GM 057073 and CA 090940. Additional funding is acknowledged from the Beckman Foundation (R.S.), the Merck/MIT consortium (Z.S.), and NIH/MIT Toxicology Training Grant 5T32GM08334 (J.R.M.).

* To whom correspondence should be addressed. Telephone: 617-258-9494. Fax: 617-258-9409.

‡ Division of Biological Engineering, Massachusetts Institute of Technology.

§ Department of Chemistry, Massachusetts Institute of Technology.

|| Department of Molecular and Cell Biology, University of Aberdeen.

⊥ Present address: Grampian Enzymes, Nisthouse Harray, Orkney KW17 2LQ, U.K.

Division of Health Sciences and Technology, Massachusetts Institute of Technology.

[1] Abbreviations: Δ4,5, Δ4,5 unsaturated glycuronidase; $\Delta4,5^{\Delta20}$, Δ4,5 glycuronidase lacking the first 20 amino acids; HSGAGs, heparin/heparan sulfate glycosaminoglycans; MALDI-MS, matrix-assisted laser desorption ionization−mass spectroscopy; DiS, disaccharide. Monosaccharides are abbreviated with the following notation: ΔU, unsaturated uronic acid; H, hexosamine; Gal, galactosamine. Subscripts 2S and 6S indicate 2-O- and 6-O-sulfation, respectively; NS and NAc indicate sulfation and acetylation of the N-position of the hexosamine.

10.1021/bi012147o CCC: $22.00
Published on Web 05/16/2002

capillary electrophoresis/MALDI-MS analyses carried out within a bioinformatics framework (*13*). We have used this method to rapidly sequence biologically important HSGAGs, including saccharide sequences involved in modulating anticoagulation (*14*). The use of additional glycosaminoglycan-degrading enzymes will increase the analytical scope of this and other sequencing procedures.

Flavobacteria synthesize many glycosaminoglycan-degrading enzymes as an integral part of their catabolic life cycle (*15*). For this reason, this particular soil bacterium has been invaluable for identifying several enzymes potentially useful to the in vitro characterization of glycosaminoglycan structure. The biosynthesis of many of these enzymes can be induced severalfold under growth conditions of high glycosaminoglycan content (*16*, *17*). One of the first such heparin-degrading enzymes purified from adapted *Flavobacterium heparinum*[2] cultures included the heparin lyases (i.e., heparinases) (*16*), which cleave large chains of heparin and heparan sulfate into constituent oligosaccharides, each possessing a Δ4,5 unsaturated uronidate at the nonreducing end. In a likewise manner, an unusual glycuronidase that specifically hydrolyzes this unsaturated uronic acid was also identified and partially purified (*18*).

In this study, we report the first known molecular cloning of the Δ4,5 glycuronidase from the *F. heparinum* genome and its subsequent recombinant expression in *Escherichia coli* as a soluble, highly active enzyme. We also present a biochemical characterization of the glycuronidase that includes a demonstration of its kinetic equivalence to the native enzyme and a description of its unusual substrate specificity.

MATERIALS AND METHODS

Chemicals and Reagents. Unless otherwise stated, biochemicals were purchased from Sigma-Aldrich Chemical Co. (St. Louis, MO). Unsaturated disaccharides were purchased from Calbiochem (San Diego, CA). Reagents for λZAP II genomic library construction and screening were obtained from Stratagene (La Jolla, CA). Additional molecular cloning reagents were obtained from the manufacturers listed.

Bacterial Strains and Growth Conditions. F. heparinum (*Cytophaga heparina*) was obtained as a lyophilized stock from American Type Culture Collection (ATCC, Manassas, VA), stock no. 13125. *E. coli* strains included TOP10 (Invitrogen, Carlsbad, CA) for PCR cloning and subcloning and BL21(DE3) (Novagen, Madison, WI) for recombinant protein expression. Bacteriophage host strains XL1-Blue MRF′ and SOLR were obtained from Stratagene.

Large-Scale Purification of Δ4,5 Glycuronidase from Flavobacterium. The Δ4,5 glycuronidase was purified from a 10 L fermentation culture essentially as described for the flavobacterial 2-*O*-sulfatase (*19*). Briefly, the cell pellet was harvested by centrifugation, resuspended in 200 mL of sodium phosphate buffer, pH 7.0, and lysed by repeated passage through an Aminco French pressure cell. The bacterial lysate was chromatographed on a CM-Sepharose CL-6B column (17 × 3.2 cm), equilibrated with 10 mM sodium phosphate, pH 6.5. Δ4,5 glycuronidase activity was eluted using a salt gradient of 0−0.3 M NaCl. Pooled fractions were diluted in sodium phosphate, pH 6.7, buffer and applied to hydroxyapatite (Bio-Gel HTP, 16 × 2 cm). Glycuronidase activity was eluted by application of a 0.01−0.5 M sodium phosphate gradient. Pooled enzyme fractions were desalted using Sephadex G-50M before being applied to a taurine−Sepharose CL-4B column (14 × 2 cm). As a final purification step, the flow-through from taurine−Sepharose chromatography was reapplied to a CM-Sepharose column and eluted by a NaCl gradient as described. Purification to homogeneity was verified by SDS−PAGE, which indicated a single protein with an apparent molecular mass of approximately 45 kDa.

Generation of Glycuronidase Peptides and Protein Sequencing. Δ4,5 glycuronidase (approximately 1 nmol) was denatured in 50 μL of 8 M urea and 0.4 M ammonium bicarbonate and reduced with 5 mM dithiothreitol at 65 °C, cooled to room temperature, and alkylated with 10 mM iodoacetic acid for 20 min. The reaction was quenched with water. To this reaction was added 4% (w/w) of trypsin, and the digestion was carried out at 37 °C overnight. The resulting peptides were separated using gradient reverse-phase HPLC (2−80% acetonitrile in 0.1% trifluoroacetic acid) over the course of 120 min. Tryptic peptides were monitored at 210 and 277 nm. Peptide peaks were collected and sequenced using an on-line Model 120 phenylthiohydantoin derivative analyzer (Biopolymers Laboratory, Massachusetts Institute of Technology).

Molecular Cloning of the Δ4,5 Glycuronidase Gene from F. heparinum Genomic DNA. Flavobacterial genomic DNA was isolated from a 10 mL flavobacterial culture using the Qiagen DNeasy DNA purification kit according to the manufacturer's instructions for Gram-negative bacteria (approximately 2×10^9 cells per column). Following purification, genomic DNA was ethanol precipitated and resuspended in TE buffer (10 mM Tris, pH 7.5, 1 mM EDTA) at 0.5 mg/mL. The quality of genomic DNA was confirmed spectrophotometrically at 260/280 nm and by electrophoresis on a 0.5% agarose gel.

The following degenerate primers were synthesized from peptides corresponding initially to peaks 19 and 24: 5′ GARACNCAYCARGGNYTNACNAAYGAR 3′ (peak 19 forward); 5′ YTCRTTNGTNARNCCYTGRTGNGTYTC 3′ (peak 19 reverse); 5′ AAYTAYGCNGAYTAYTAYTAY 3′ (peak 24 forward); 5′ RTARTARTARTCNGCRTARTT 3′ (peak 24 reverse). All four primers were screened in a PCR assay using all possible pairings (forward and reverse). The PCR reaction conditions included 200 ng of genomic DNA, 200 pmol for each forward and reverse primer, 200 μM dNTPs, and 1 unit of Vent DNA polymerase (New England Biolabs) in a 100 μL reaction volume. A total of 35 cycles were completed using a 52 °C annealing temperature and 2 min extensions at 72 °C. A 450 bp product amplified using primers 19 forward and 24 reverse was gel purified and subjected to direct DNA sequencing, which confirmed the inclusion of the translated sequence corresponding to peptide peaks 19 and 24 in addition to peak 12. The same DNA was also ^{32}P radiolabeled by random priming using 200 μCi of [α-^{32}P]dCTP at 6000 Ci/mmol (NEN, Boston, MA), 50−100 ng of DNA, and the Prime-it II random priming kit (Stratagene) (probe 1). Unincorporated [^{32}P]dNTPs were removed by gel filtration using G-50 Quick-spin columns (Roche Biochemicals, Piscataway, NJ).

[2] While *Flavobacterium heparinum* is the historical (and commonly used) taxonomy, the current scientific name for this microorganism is *Cytophaga heparina*.

DNA hybridization probe 2 was initially created by PCR as described above except using degenerate primers 26 (CARACNTAYACNCCNGGNATGAAY) (peak 26 forward) and 20 pmol of reverse, nondegenerate primer 54 (TTCATGGTCGTAACCGCATG). Direct sequencing of this PCR fragment confirmed the presence of the gene sequence corresponding to peak 26 and peak 13 peptides. Δ4,5 5′-specific DNA probe 3 used in DNA southern hybridizations (below) was PCR amplified from genomic DNA using primers 68 (TATACACCAGGCATGAACCC)) and 74 (CCCAGTATAAATACTCCAGGT).

Plaque Hybridization Screening of the F. heparinum Genomic Library. A λZAP II genomic library was constructed as described (*20*). The amplified library (1×10^{10} pfu/mL) was plated out at approximately 1×10^6 pfu (~50000 pfu per plate) on 100 × 150 mm LB plates. Plaque lifts onto nylon membranes (Nytran Supercharge, Schleicher and Schuell) and subsequent hybridization screenings were completed using standard methods and solutions (*21*). DNA was cross-linked to each filter by UV irradiation (Stratagene Stratalinker) for 30 s at 1200 J/cm^3. Hybridizations were carried at 42 °C using 10^7-10^8 cpm of radiolabeled probe (at approximately 0.25 ng/mL). Low stringency washes were carried out at room temperature in 2× SSC and 0.1% SDS; high stringency washes carried out at 58−60 °C in 0.2× SSC and 0.1% SDS. Hybridized plaques were visualized by phosphorimaging (Molecular Dynamics) and/or ^{32}P autoradiography. Tertiary screens of positive clones were completed, and the recombinant phage was excised as a double-stranded phagemid (pBluescript) using the Ex-Assist interference-resistant helper phage according to the manufacturer's protocol (Stratagene). Recombinants were characterized by DNA sequencing using both T7 and T3 primers.

Creation of a Flavobacterium BglII−EcoRI Subgenomic Library for Isolation of the Δ4,5 5′ Terminus. Southern DNA hybridizations were completed according to standard protocols (*21*) using ^{32}P-radiolabeled probe 3. One microgram of genomic DNA was cut with 20 units of *Eco*RI, *Bgl*II, and *Hin*dIII individually or as double digests, and the restriction products were resolved by gel electrophoresis on a 1% agarose gel run in 1× TAE buffer. On the basis of this Southern analysis, a 1.5 kb DNA fragment containing the Δ4,5 5′ terminus was identified. Ten micrograms of flavobacterial genomic DNA was therefore digested with *Bgl*II−*Eco*RI and the DNA resolved on a preparative gel run under conditions identical to those described for the analytical gel. DNA ranging from approximately 1−2 kb was gel purified and ligated into pLITMUS as a *Bgl*II−*Eco*RI cassette. Positive clones were identified by PCR colony screening using primers 68 and 74 and confirmed by DNA sequencing.

PCR Cloning of the Δ4,5 Gene and Recombinant Expression in E. coli. The full-length glycuronidase gene was directly PCR amplified from genomic DNA using forward primer 85 (TGTTCTAGA**CATATG**AAATCACTACTCAGTGC) and reverse primer 86 (GT**CTCGAG**GATCCTTAAGACTGATTAATTGTT) (with *Nde*I and *Xho*I restriction sites denoted in bold), 200 ng of genomic DNA, and Vent DNA polymerase for 35 cycles. dA overhangs were generated in a final 10 min extension at 72 °C using AmpliTaq DNA polymerase (Applied Biosystems). PCR products were gel purified, ligated into the TOPO/TA PCR cloning vector (Invitrogen), and transformed into one-shot TOP10 chemically competent cells. Positive clones were identified by blue/white colony selection and confirmed by PCR colony screening. The 1.2 kb Δ4,5 gene was subcloned into expression plasmid pET28a (Novagen) as an *Nde*I−*Xho*I cassette. Final expression clones were confirmed by plasmid DNA sequencing.

For the expression of Δ4,5 glycuronidase beginning with M21 (Δ4,5$^{\Delta 20}$), the forward primer 95 (TGTTCTAGA-**CATATG**ACAGTTACGAAAGGCAA) (also containing an *Nde*I restriction site near its 5′ terminus) was used in place of primer 85 (above). Fifty nanograms of the original expression plasmid pET28a/Δ4,5 was used as the DNA template in PCR reactions involving a total of 20 cycles. Otherwise, cloning was as described for the full-length gene. Both pET28a/Δ4,5 and pET28aΔ4,5$^{\Delta 20}$ plasmids were transformed into BL21(DE3) for expression as N-terminal 6× His-tagged proteins. One liter cultures were grown at room temperature (~20 °C) in LB media supplemented with 40 μg/mL kanamycin. Protein expression was induced with 500 μM IPTG added at an A_{600} of 1.0. Induced cultures were allowed to grow for 15 h (also at room temperature).

Recombinant Δ4,5 Glycuronidase Purification. Bacterial cells were harvested by centrifugation at 6000*g* for 20 min and resuspended in 40 mL of binding buffer (50 mM Tris-HCl, pH 7.9, 0.5 M NaCl, and 10 mM imidazole). Lysis was initiated by the addition of 0.1 mg/mL lysozyme (20 min at room temperature) followed by intermittent sonication in an ice−water bath using a Misonex XL sonicator at 40−50% output. The crude lysate was fractionated by low-speed centrifugation (20000*g*, 4 °C, 15 min), and the supernatant was filtered through a 0.45 μm filter. The 6× His-tagged Δ4,5 glycuronidase was purified by Ni^{2+} chelation chromatography on a 5 mL Hi-Trap column (Pharmacia Biotech) precharged with 200 mM $NiSO_4$ and subsequently equilibrated with binding buffer. Column washes included an intermediate step with 50 mM imidazole. The Δ4,5 enzyme was eluted from the column in 5 mL fractions using high imidazole elution buffer (50 mM Tris-HCl, pH 7.9, 0.5 M NaCl, and 250 mM imidazole). Peak fractions were dialyzed overnight against 4 L of phosphate buffer (0.1 M sodium phosphate, pH 7.0, 0.5 M NaCl) to remove the imidazole.

The 6× His tag was effectively cleaved by adding biotinylated thrombin at 2 units/milligram of recombinant protein, overnight at 4 °C with gentle inversion. Thrombin was captured by binding to streptavidin−agarose at 4 °C for 2 h using the Thrombin Capture Kit (Novagen). The cleaved peptide MGSSHHHHHHSSGLVPR was removed by final dialysis against a 1000-fold volume of phosphate buffer.

Protein concentrations were determined by the Bio-Rad protein assay and confirmed by UV spectroscopy using a theoretical molar extinction coefficient $\epsilon = 88900$ for Δ4,5$^{\Delta 20}$. Protein purity was assessed by SDS−PAGE followed by Coomassie Brilliant Blue staining.

Computational Methods. Signal sequence predictions were made by SignalP V.1.1 using the von Heijne computational method (*22*) with maximum *Y* and *S* cutoffs set at 0.36 and 0.88, respectively. Glycuronidase multiple sequence alignments were made from select BLASTP database sequences (with scores exceeding 120 bits and less than 6% gaps) using the CLUSTAL W program (version 1.81) preset to an open

gap penalty of 10.0, a gap extension penalty of 0.20, and both hydrophilic and residue-specific gap penalties turned on.

Assay for Enzyme Activity and Determination of Kinetic Parameters. Standard reactions were carried out at 30 °C and included 100 mM sodium phosphate buffer, pH 6.4, 50 mM NaCl, 500 μM disaccharide substrate, and 200 nM enzyme in a 100 μL reaction volume. Hydrolysis of unsaturated heparin disaccharides was determined spectrophotometrically by measuring the loss of the Δ4,5 chromophore measured at 232 nm. Substrate hydrolysis was calculated using the following molar extinction coefficients empirically determined for each unsaturated disaccharide substrate: ΔUH_{NAc}, $\epsilon_{232} = 4524$; $\Delta UH_{NAc,6S}$, $\epsilon_{232} = 4300$; ΔUH_{NS}, $\epsilon_{232} = 6600$; $\Delta UH_{NS,6S}$, $\epsilon_{232} = 6075$; $\Delta UH_{NH2,6S}$, $\epsilon_{232} = 4826$; $\Delta U_{2S}H_{NS}$, $\epsilon_{232} = 4433$. Initial rates (V_0) were extrapolated from linear activities representing <10% substrate turnover and fit to pseudo-first-order kinetics. For kinetic experiments, the disaccharide concentration for each respective substrate was varied from 48 to 400 μM concentrations. K_m and k_{cat} values were extrapolated from V_0 vs [S] curves fit to the Michaelis−Menten equation by a nonlinear least squares regression.

For experiments measuring the relative effect of ionic strength on glycuronidase activity, the NaCl concentration was varied from 0.05 to 1 M in 0.1 M sodium phosphate buffer (pH 6.4), 200 μM $\Delta UH_{NS,6S}$, and 100 nM enzyme under otherwise standard reaction conditions. The effect of pH on catalytic activity was kinetically determined at varying $\Delta UH_{NS,6S}$ concentrations in 100 mM sodium phosphate buffer at pH 5.2, 5.6, 6.0, 6.4, 6.8, 7.2, and 7.8. Data were fit to Michaelis−Menten kinetics as described above and the relative k_{cat}/K_m ratios plotted as a function of pH.

Detection of Δ4,5 Glycuronidase Activity by Capillary Electrophoresis. Two hundred micrograms of heparin (Celsus Laboratories) was subjected to exhaustive heparinase digestion as described (*13*) with certain modifications that included a 50 mM PIPES buffer, pH 6.5, with 100 mM NaCl in a 100 μL reaction volume. Following heparinase treatment, 25 pmol of Δ4,5 glycuronidase was added to one-half of the original reaction (preequilibrated at 30 °C). Twenty microliter aliquots were removed at 1 and 30 min, and activity was quenched by heating at 95 °C for 10 min. Twenty microliters of the minus Δ4,5 control (also heated for 10 min) was used as the 0 time point. Unsaturated disaccharide products were resolved by capillary electrophoresis run for 25 min under positive polarity mode as previously described (*12*).

Molecular Mass Determinations by MALDI-MS. The molecular mass of both the wild-type and recombinantly expressed forms of the enzyme was determined by matrix-assisted laser desorption ionization−mass spectrometry (MALDI-MS) using a Voyager Elite time-of-flight instrument (PerSeptive Biosystems, Framingham, MA). Prior to mass analysis, the N-terminal histidine tag of the recombinant protein was removed. For MALDI-MS analysis, 0.5 μL of an aqueous protein solution (0.1−1 mg/mL) was added to the target followed by the addition of 1 μL of a saturated sinapinic acid matrix solution in 50% acetonitrile/water. The sample was allowed to air-dry and then placed into the instrument. Mass spectra were collected in the linear mode using delayed extraction. Instrument parameters were adjusted to maximize the signal. All spectra were calibrated externally using a mixture of ovalbumin and carbonic anhydrase (Sigma-Aldrich).

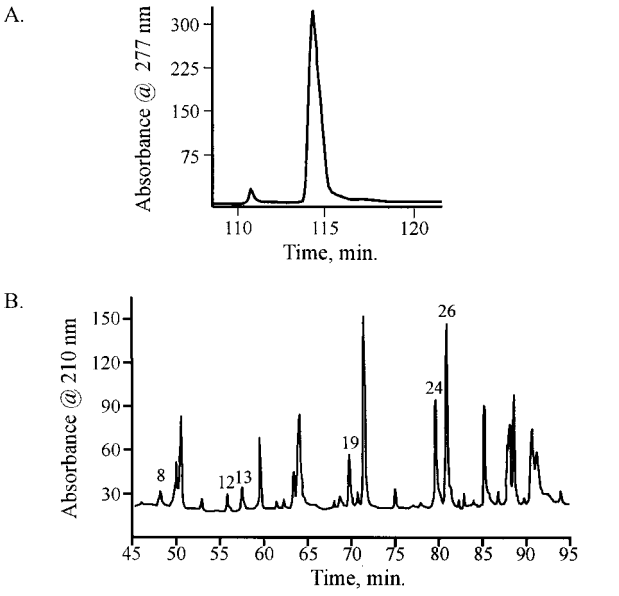

C.

Peak No.	Peptide Sequence
8	EFNKPEWFDAAK
12	PGENQFFILK
13	FTLALDTIQYVK
19	VLQRETHQGLTNESAWARGQAWGLYGYTMSYK
24	HSVGALLYNSEIDTPLNYADYYYLEALK
26	TAVIQLTRAAQTYTPGMNPRSVNPDGTVRLAPPR

FIGURE 1: Purification of Δ4,5 glycuronidase from *Flavobacterium* and resultant proteolytic products. (A) C18 chromatogram of the purified enzyme. (B) Purification of Δ4,5 peptides by reverse-phase HPLC following trypsinization of the native protein. (C) Amino acid sequence of select peptides isolated in (B).

RESULTS

Molecular Cloning of the Δ4,5 Glycuronidase Gene from the F. heparinum Genome. To clone the Δ4,5 glycuronidase gene, we isolated a series of Δ4,5 glycuronidase-derived peptides after a protease treatment of the purified enzyme. The native enzyme was directly purified from fermentation cultures of *F. heparinum* using a five-step chromatography scheme as previously described (*19*). The extent of purity was ultimately characterized by reverse-phase chromatography, which indicated a single major peak (Figure 1A). We were able to generate a number of peptides by a limit trypsin digestion of the purified enzyme. A total of 26 peptide fragments were resolved by reverse-phase chromatography (Figure 1B). From these 26, at least eight peptides (corresponding to major peaks 8, 12, 13, 19, 24, and 26) were of sufficient yield and purity and were selected for protein sequence determination (Figure 1C).

On the basis of this information, we designed degenerate primers corresponding to peaks 19, 24, and 26. These primers were used to PCR amplify Δ4,5 specific sequences to be used as suitable DNA hybridization probes for screening the flavobacterial genomic library. A combination of two primer pairs in particular (peak 19 forward and peak 24 reverse) gave a discrete PCR product of approximately 450 base pairs (data not shown). The translation of the corresponding DNA sequence indicated that it contained the expected amino acid

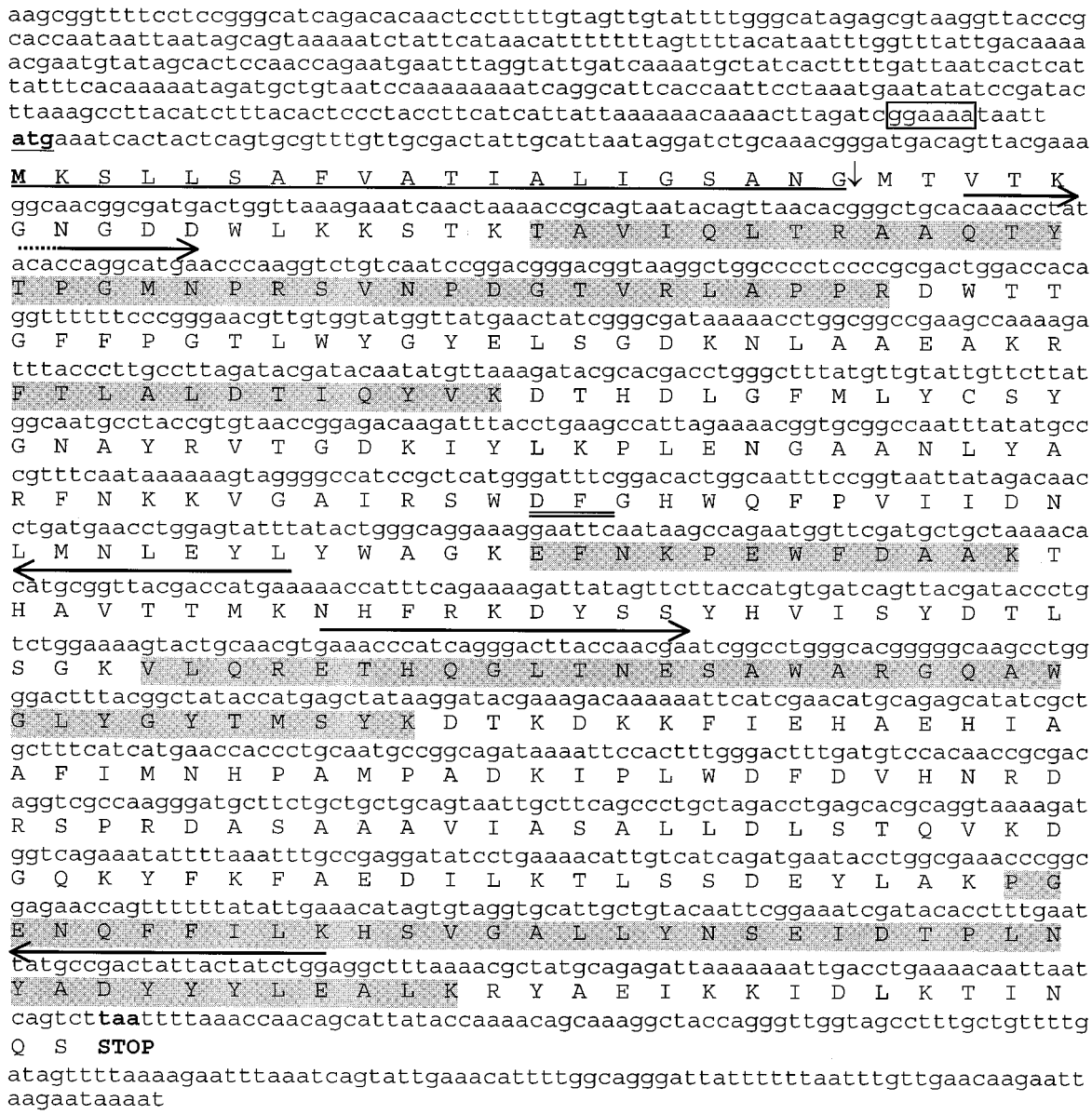

FIGURE 2: Δ4,5 glycuronidase gene sequence. The full-length gene was isolated by PCR as described in Materials and Methods. Shown here are both the coding and flanking DNA sequences. The coding sequence of 1209 base pairs contains an ORF encoding a putative protein of 402 amino acids. Initiation and termination codons are highlighted in bold. The possible Shine−Dalgarno (SD) sequence is boxed. The presumed signal sequence is underlined and its cleavage site delimited by a vertical arrow. The *Eco*RI restriction site is double overscored. Also shown are the degenerate primer pairs (shown as arrows) used to PCR amplify DNA hybridization probes 1 and 2 as well as the relative positions of purified Δ4,5 peptides (shaded in gray) for which direct sequence information was obtained.

sequence corresponding to peaks 19 and 24. The peak 12 peptide also mapped to this region. We used this PCR DNA fragment in the initial plaque hybridizations. The most 5′-terminal clone obtained in this screening included approximately one-half of the predicted gene size corresponding to the carboxy terminus of the putative ORF. Invariably, all of the isolated clones possessed an *Eco*RI site at their respective 5′ termini. In an attempt to isolate a clone from the phage library possessing the other half of the gene, we rescreened additional plaques, this time using a second N-terminal specific DNA hybridization probe (probe 2) in tandem with the original probe 1. This second strategy also failed to yield any clones with the fully intact Δ4,5 gene.

Alternate approaches were taken in an attempt to obtain the 5′ terminus of the glycuronidase gene. The size of this missing region, based on the molecular mass of the native protein, was estimated to be approximately 45 amino acids (135 base pairs). We completed DNA southern analyses to identify potentially useful DNA restriction sites flanking the 5′ end of the Δ4,5 gene. This restriction mapping ultimately involved the use of the *Eco*RI site within the gene in conjunction with hybridization probe 3 (whose 3′ end lies just 5′ to this restriction site) to positively bias our search for the remaining amino terminus. On the basis of this refined map, we successfully isolated and subcloned an approximately1.5 kb *Bgl*II−*Eco*RI Δ4,5 fragment into pLITMUS. The 5′ terminus of the Δ4,5 gene was obtained from direct DNA sequencing of this subgenomic clone.

A summary of the full-length gene sequence (compiled from the two overlapping cloning methods) is depicted in Figure 2. The Δ4,5 coding sequence is comprised of 1209 base pairs corresponding to an ORF that encodes a 402 amino

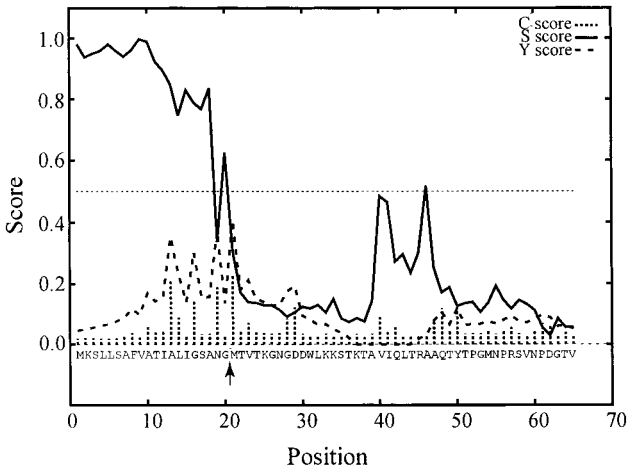

FIGURE 3: Assignment of a putative Δ4,5 glycuronidase signal sequence. Theoretical signal sequence determination using amino acids 1−65. Indices were calculated using SignalP V.1.1 using networks trained on Gram-negative bacteria. A vertical arrow indicates the putative cleavage site located between G20 and M21.

acid protein. The predicted molecular mass of 45621 Da for the translated protein corresponds very well with an empirical molecular mass of 45586 Da for the purified flavobacterial enzyme determined by MALDI-MS (data not shown). All of the peptides for which we obtained sequence information map to this Δ4,5 ORF. On the basis of further primary sequence analyses, we have also identified a likely bacterial signal sequence spanning amino acids 1−20 also possessing a putative cleavage site between residues G20 and M21 (Figure 3). The presence within this hydrophobic amino terminus of an **A**XX**A** peptidase cleavage motif further supports this presumption (*24*).

A search for related sequences in the NCBI protein database led to several functionally related enzymes. In a multiple sequence alignment of our cloned enzyme with select unsaturated glucuronyl hydrolases, we found a homology that generally corresponded to upward of 30% identity and nearly 50% similarity at the primary sequence level (Figure 4). This relatedness spanned most of the enzyme sequence, excluding the N-terminus. On the basis of this alignment, we found several highly conserved positions within the *F. heparinum* Δ4,5 glycuronidase that included several aromatic and acidic residues, e.g., W73, F77, Y86, F119, W162, W244, W250, Y253 W292, and Y379; D116, D174, D213, D287, D293, D305, D371, and D378. Other invariant amino acids of possible catalytic importance include H115, H201, H218, and basic residues R151, R211, and R246.

Recombinant Expression and Purification of the Δ4,5 Glycuronidase. Using PCR, we cloned from the *F. heparinum* genome both the full-length enzyme and the "mature" enzyme lacking the N-terminal 20 amino acid signal sequence ($\Delta4,5^{\Delta20}$) into a T7-based expression plasmid. Cloning into pET28a permitted the expression of the glycuronidase as an N-terminal 6× His-tagged fusion protein. Pilot expression studies focused on the full-length enzyme. In these initial experiments, we examined several different induction conditions such as temperature, time and length of induction, and even IPTG concentrations. In every case, the full-length enzyme was present nearly exclusively as an insoluble fraction. Attempts to purify the enzyme directly

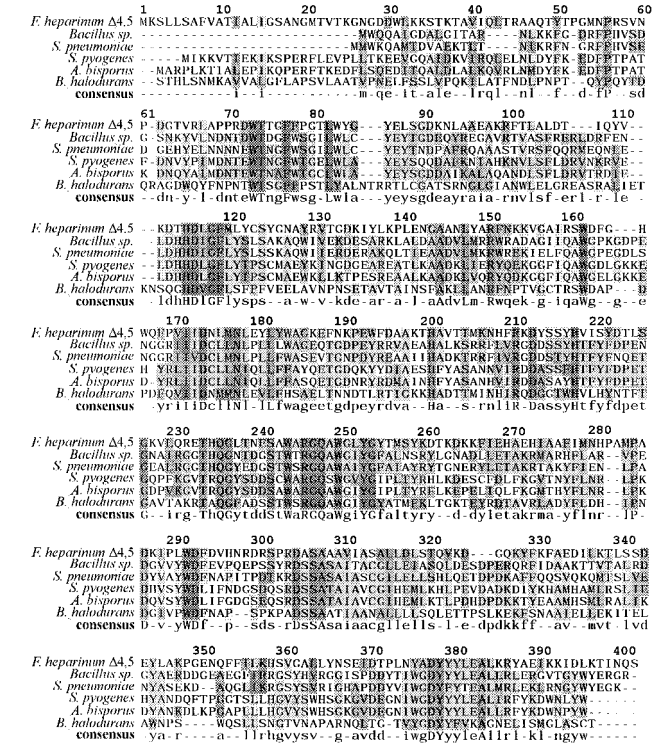

FIGURE 4: CLUSTAL W multiple sequence alignment of Δ4,5 glycuronidase and select unsaturated glucuronyl hydrolases. Protein sequences were selected from an initial BLASTP search of the protein database. Identical amino acids are shaded in dark gray and conservative substitutions in light gray. GenBank accession numbers are as follows: *Bacillus* sp. (AB019619); *Streptococcus pneumoniae* (AE008410); *Streptococcus pyogenes* (AE006517); *Agaricus bisporsus* (AJ271692); *Bactobacillus halodurans* (AP001514).

from inclusion bodies and then refold the protein were not successful. Solubility was partially achieved by a combined use of detergents (e.g., CHAPS), increasing salt concentrations, and the addition of glycerol; the partially purified enzyme, however, was largely inactive. Conversely, recombinant expression of the enzyme lacking the presumed signal sequence yielded remarkably different results. In this case, soluble recombinant expression levels routinely reached several hundred milligrams of protein per liter of induced cells. The specific activity of this enzyme on the heparin disaccharide ΔUH_{NAc} was likewise robust (see below).

A summary of the expression and purification of $\Delta4,5^{\Delta20}$ is shown in Figure 5 and Table 1. A two-step purification comprised of Ni^{2+} chelation chromatography followed by thrombin cleavage to remove the 6× His purification tag typically yielded over 200 mg of pure enzyme as assessed by SDS−PAGE followed by Coomassie Brilliant Blue staining. Most notably, the specific activity of the recombinant enzyme acting upon ΔUH_{NAc} far exceeded the values reported in the literature for the wild-type enzyme (*18*). While removal of the 6× His tag from the N-terminus of the enzyme was unnecessary for optimal hydrolytic activity, the presence of the histidine tag did appear to instigate protein precipitation over an extended time period, especially at higher enzyme concentrations. This tag was, therefore, removed for all subsequent biochemical experiments. In this manner, the recombinant protein was stable at 4 °C for at least 2 weeks, during which time it remained in solution at protein concentrations exceeding 10 mg/mL under the buffer conditions described.

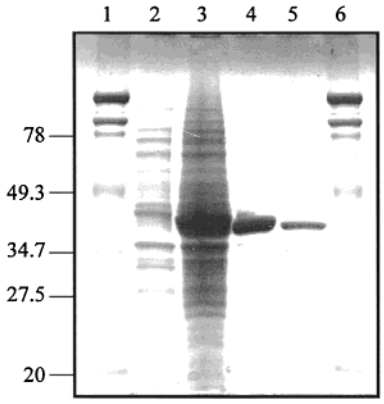

FIGURE 5: Recombinant $\Delta 4,5^{\Delta 20}$ protein expression and purification. SDS−PAGE of Δ4,5 protein fractions at various purification stages following expression in BL21(DE3) as a 6× His N-terminal fusion protein. Shown here is a 12% gel stained with Coomassie Brilliant Blue. Lanes: 2, lysate from uninduced bacterial cells; 3, crude cell lysate from induced cultures; 4, Ni^{2+} chelation chromatography purification; 5, thrombin cleavage to remove the N-terminal 6× His purification tag. Molecular mass markers (lanes 1 and 6) are also noted.

Table 1: Purification Summary for the Recombinant Δ4,5 Glycuronidase[a]

purification step	protein yield (mg)	specific activity [μmol of DiS min^{-1} (mg of protein)$^{-1}$]	*x*-fold purification
crude lysate	400	4.7	
Ni^{2+} chromatography	205	12.9	2.7
thrombin cleavage	205	13.6	2.9

[a] Specific activities for each fraction were measured using 800 ng of protein and 120 μM unsulfated heparin disaccharide (DiS) ΔUH_{NAc} in a 100 μL reaction volume. The *x*-fold purification was calculated relative to the specific activity measured for the crude lysate.

A molecular mass of 44209 Da was determined for the recombinant enzyme (i.e., $\Delta 4,5^{\Delta 20}$) by MALDI-MS. This empirically established molecular mass is consistent with its theoretical value of 43956 Da, based on its amino acid composition. This value physically differs by 1377 Da in comparison to a molecular mass of 45586 Da likewise measured for the native enzyme. This mass differential is largely accounted for by the engineered removal in the recombinant protein of the 20 amino acid signal sequence. However, we cannot exclude the possibility of differential posttranslational modifications such as glycosylation largely accounting for the observed differences between the two enzyme populations. Unfortunately, chemical blocking precluded us from determining the N-terminal sequence of the native protein.

Biochemical Conditions for Optimal Enzyme Activity. To determine the optimal reaction conditions for Δ4,5 glycuronidase activity, we analyzed initial reaction rates as a function of buffer, pH, temperature, and ionic strength (Figure 6). For these experiments, we used the unsaturated, disulfated heparin disaccharide substrate $\Delta UH_{NS,6S}$. On the basis of what is known about the degradation of heparin/heparan sulfate-like glycosaminoglycans by flavobacteria (*25*) as well as initial biochemical characterization of this and related enzymes (*18, 26*), we hypothesized that an unsaturated heparin disaccharide would be a logical substrate for the Δ4,5 glycuronidase. Enzyme activity was routinely monitored by a loss of absorbance at 232 nm, corresponding

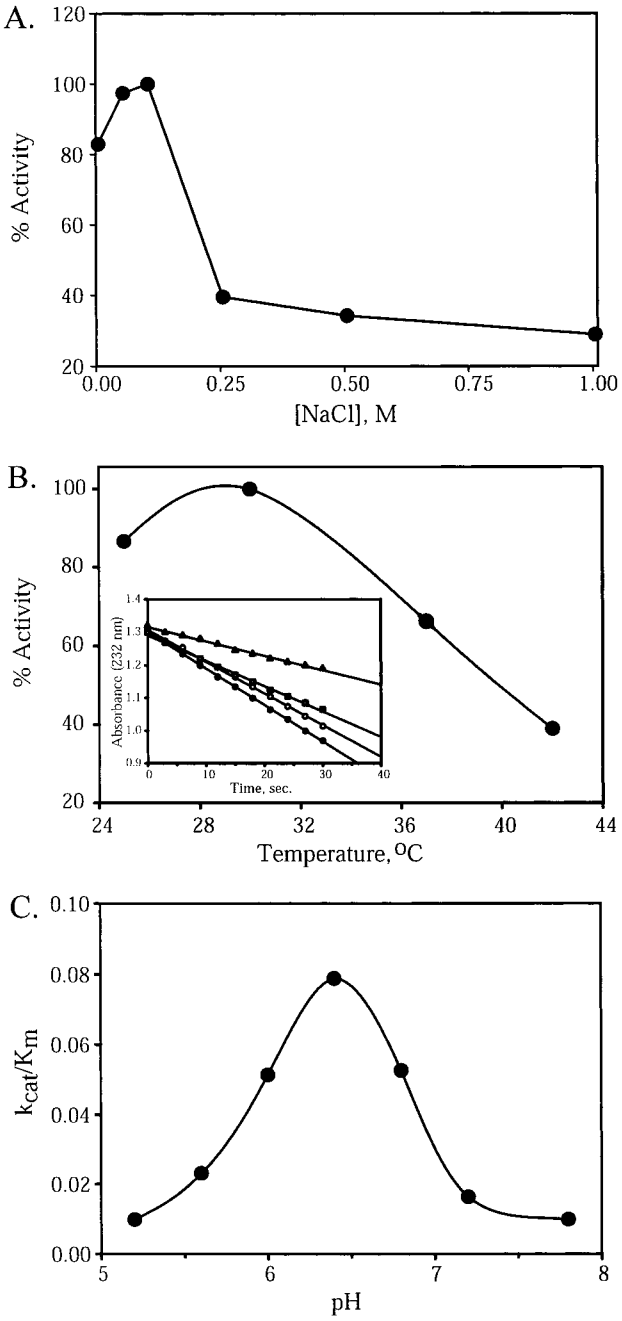

FIGURE 6: Δ4,5 glycuronidase biochemical reaction conditions. (A) NaCl titration. (B) Effect of reaction temperature. Inset B: Δ4,5 glycuronidase reaction rates measured at varying temperatures by the disappearance of UV absorbance (232 nm): 25 °C (○); 30 °C (●); 37 °C (□); 42 °C (▲). Relative enzyme activities in (A) and (B) were derived from initial rates and were normalized to 100% activity represented by 100 mM NaCl and 30 °C, respectively. (C) pH profile. K_m and k_{cat} values for the pH profile were extrapolated from Michaelis−Menten kinetics as described in Materials and Methods. The disulfated heparin disaccharide $\Delta UH_{NS,6S}$ was used in all three experiments.

indirectly to the hydrolysis of the uronic acid from the nonreducing end. The observed decrease in UV absorption is presumably due to the chain opening of the unsaturated uronidate monosaccharide concomitant with keto−enol isomerization to form the α-keto acid, resulting in the loss of the λ_{232}-absorbing carbon−carbon bond (*27*).

Under the examined conditions, we observed a NaCl concentration−activity dependence with optimal enzymatic

activity occurring at salt concentrations between 50 and 100 mM. At concentrations exceeding 100 mM NaCl, the enzyme demonstrated a significant decrease in activity that was sharply dependent on the ionic strength (Figure 6A), i.e., with approximately 60% inhibition occurring at 250 mM NaCl relative to 100% activity measured at 100 mM NaCl.

The observed pH profile for the glycuronidase was bell-shaped (Figure 6B) with a pH optimum of 6.4. This result is consistent with previously published results (*18*). In addition, temperature titration experiments indicated that maximal enzymatic activity for the Δ4,5 glycuronidase was achieved at 30 °C. Interestingly, initial reaction rates were significantly reduced at higher temperatures, especially at 42 °C (Figure 6C). Precincubation experiments at 30, 37, and 42 °C to assess enzyme stability indicated no significant change in enzymatic activity when the enzyme was subsequently measured under the standard 30 °C reaction conditions (data not shown). The results of these experiments suggest that the observed decrease in the enzymatic reaction rate at higher temperatures is not due to a thermal lability of the Δ4,5 glycuronidase; rather it reflects some intrinsic property of its catalytic function.

As a final variable for optimizing Δ4,5 glycuronidase in vitro reaction conditions, we also considered any requirement for divalent metal ions, including Ca^{2+}, Mg^{2+}, Mn^{2+}, and others. We found no evidence that any metal cofactor is either required for catalysis or activates the enzyme to any appreciable extent (data not shown).

Having established the reaction conditions for optimal Δ4,5 glycuronidase activity, we next compared the specific activity of the recombinant enzyme ($\Delta4,5^{\Delta20}$) to the native enzyme purified directly from *F. heparinum*. The activities of both enzyme fractions were measured in parallel under identical reaction conditions. In this comparison, the recombinant Δ4,5 possessed a 1.5-fold higher initial velocity relative to the native enzyme (data not shown). These results demonstrate that the recombinant enzyme is comparable in activity to the native form of the enzyme and possesses the added benefit that over 1000-fold more enzyme can be obtained per liter of culture as compared to the wild type.

Δ4,5 Glycuronidase Substrate Specificity. Given the fact that the recombinant form of the Δ4,5 glycuronidase possessed similar attributes to the native form and is undoubtedly free of contaminating HSGAG-degrading activities, this form of the enzyme was used to characterize the substrate specificity of the Δ4,5 glycuronidase using various unsaturated glycosaminoglycan disaccharide substrates. These substrates examined included heparin, chondroitin, and hyaluronan disaccharides. In particular, we considered the possibility of any structural discriminations pertaining to the glycosidic linkage position (1→4 vs 1→3) and relative sulfation state within the disaccharide. For each substrate, kinetic parameters were determined on the basis of substrate saturation profiles that fit Michaelis−Menten assumptions (Figure 7). These kinetic values are listed in Table 2. For the heparin disaccharides, k_{cat} values varied significantly from approximately 2 to 15 s^{-1}, while the apparent K_m values for each respective disaccharide were comparable, ranging from approximately 100 to 300 μM. The heparin disaccharide $\Delta U_{2S}H_{NS}$ was unequivocally not a substrate at any of the concentrations studied, even following an extended incubation time spanning several hours (data not shown). For those

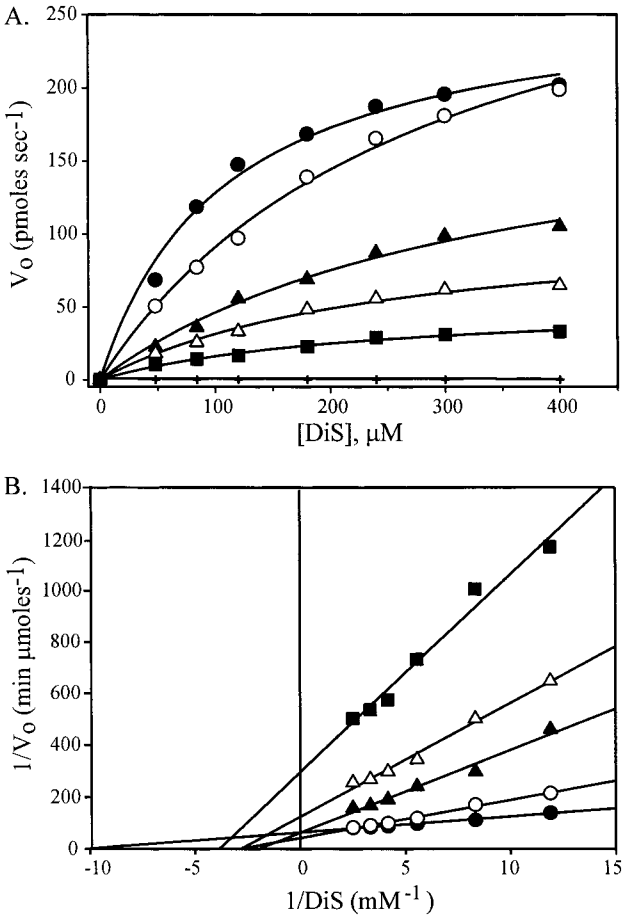

FIGURE 7: Disaccharide substrate specificity. (A) Kinetic profiles for heparin disaccharides of varying sulfation. Initial rates were determined using 200 nM enzyme under standard conditions. V_0 vs [S] curves were fit to Michaelis−Menten steady-state kinetics using a nonlinear least-squares analysis. (B) Lineweaver−Burk representation of the data shown in (A): $\Delta UH_{NAc,6S}$ (●); ΔUH_{NAc} (○); $\Delta UH_{NS,6S}$ (▲); ΔUH_{NS} (△); $\Delta UH_{NH2,6S}$ (■); $\Delta U_{2S}H_{NS}$ (+).

Table 2: Kinetic Parameters for Heparin Disaccharides[a]

disaccharide substrates	k_{cat} (s^{-1})	K_m (μM)	k_{cat}/K_m	relative k_{cat}/K_m
ΔUH_{NAc}	15.3 ± 0.9	283 ± 31	0.054	0.49
$\Delta UH_{NAc,6S}$	11.7 ± 0.6	107 ± 15	0.110	1.0
ΔUH_{NS}	4.9 ± 0.4	251 ± 40	0.020	0.18
$\Delta UH_{NS,6S}$	8.8 ± 0.9	334 ± 57	0.026	0.24
$\Delta UH_{NH2,6S}$	2.4 ± 0.2	235 ± 40	0.010	0.09
$\Delta U_{2S}H_{NS}$	NA[b]	NA	NA	NA

[a] k_{cat} and K_m values were determined from nonlinear regression analyses of the Michaelis−Menten curves presented in Figure 7. [b] NA, no activity was detected for $\Delta U_{2S}H_{NS}$.

unsaturated heparin disaccharides that were hydrolyzed under the conditions tested and for which kinetic parameters could be determined, a highly interesting substrate preference was apparent. In this hierarchy, the two disaccharides ΔUH_{NAc} and $\Delta UH_{NAc,6S}$ were clearly the best substrates. In comparison, $\Delta UH_{NH2,6S}$ and ΔUH_{NS} were relatively poor substrates. The kinetic values for $\Delta UH_{NS,6S}$ fell roughly in the middle between these two boundaries.

None of the non-heparin disaccharides were hydrolyzed under the conditions established to measure substrate kinetics. These results indicate an unequivocal discrimination of the Δ4,5 glycuronidase with regard to linkage position, with a strong preference for 1→4 versus 1→3 linkages. At the same

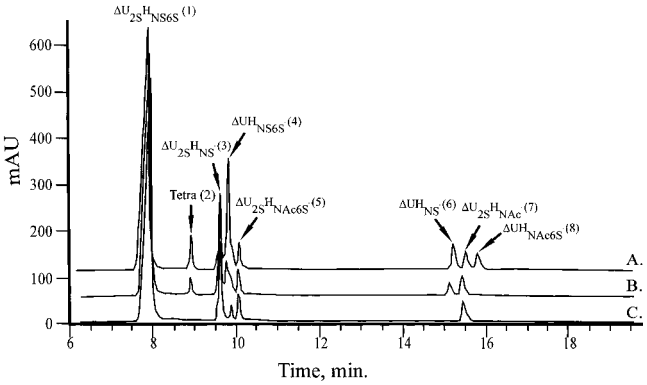

FIGURE 8: Tandem use of heparinases and Δ4,5 glycuronidase in HSGAG compositional analyses. Heparin (200 μg) was exhaustively digested with heparinases I, II, and III, after which Δ4,5 was added for a varying length of time. Unsaturated disaccharide products were resolved by capillary electrophoresis. Assignment of saccharide composition shown for each peak was confirmed by MALDI-MS. Each electrophoretogram represents varying time of Δ4,5 glycuronidase treatment: (A) minus Δ4,5 enzyme control; (B) 1 min (partial) incubation; (C) 30 min (exhaustive) incubation.

time, 1→3-containing disaccharides were hydrolyzed slowly to varying degrees when the enzyme reactions were conducted over a much longer time course (>12 h) and at considerably higher enzyme concentrations (data not shown). After approximately 18 h, greater than 80% of a monosulfated chondroitin disaccharide ($\Delta UGal_{NAc,6S}$) was hydrolyzed, whereas the nonsulfated chondroitin ($\Delta UGal_{NAc}$) and the hyaluronan disaccharide (ΔUH) were still present at approximately 40% and 65%, respectively. The apparently positive effect of chondroitin 6-O-sulfation within the galactosamine is consistent with our results for the heparin substrates and provides further evidence for the influence of this position in dictating substrate specificity.

On the basis of the clear, kinetically defined substrate specificity for the unsaturated disaccharides, we set out to validate these results while, at the same time, investigating the utility of the Δ4,5 glycuronidase as an enzymatic tool for HSGAG compositional analysis. In this manner, the Δ4,5 glycuronidase could potentially be very useful in assessing the composition of disaccharides resulting from prior heparinase treatment of heparin/heparan sulfate. For this particular experiment, we pretreated 200 μg of heparin with a heparinase cocktail. This exhaustive digestion was then directly followed by a relatively short (1 min) or long (30 min) Δ4,5 glycuronidase treatment carried out under optimal reaction conditions. The unsaturated disaccharide products were then resolved by capillary electrophoresis. The electrophoretic mobility profile for the Δ4,5 glycuronidase-treated saccharides was then directly compared to the untreated control (i.e., heparinase treatment only) run under identical conditions (Figure 8). Seven disaccharide peaks were present in the capillary electrophoretogram corresponding to the heparinase only control (Figure 8A). A structural assignment for each one of these peaks was made on the basis of previously established compositional analyses (data not shown). Consistent with the observed substrate specificity for the Δ4,5 glycuronidase, the relative area of the peaks corresponding to 2-O-containing disaccharides remained unchanged over the time course of the experiment (>18 h). On the other hand, peaks corresponding to disaccharides lacking the 2-O sulfate were eliminated to various extents over the course of the experiment. The relative rates of their disappearances corresponded exactly to their substrate preference as determined in the previous kinetic experiment. $\Delta UH_{NAc,6S}$ (peak 8) was essentially hydrolyzed within 1 min; $\Delta UH_{NS,6S}$ (peak 4) and ΔUH_{NS} (peak 6) were hydrolyzed approximately 75% and 50%, respectively. These two latter substrates were completely depleted by 30 min.

In addition to the assigned disaccharides, the Δ4,5 glycuronidase also acted on a heparinase-generated tetrasaccharide (identified as peak 2 in Figure 8). The assignment of peak 2 as a tetrasaccharide was confirmed by MALDI-MS (data not shown), which indicated a mass of 1036.9 Da that corresponds to a singly acetylated tetrasaccharide with four sulfates. Disaccharide analysis of this tetrasaccharide further indicated that it does not contain a 2-*O*-sulfate at the nonreducing end. The Δ4,5 enzyme hydrolyzed approximately one-half of the unsaturated starting material after 1 min. The relative rate of hydrolysis for this tetrasaccharide roughly corresponded to the rate observed for the disaccharide ΔUH_{NS} (peak 6). This exciting result clearly indicates that a longer chain saccharide such as a tetrasaccharide is in fact a substrate for the Δ4,5-catalyzed hydrolysis.

DISCUSSION

In this paper, we report the first known molecular cloning of the Δ4,5 glycuronidase gene from *F. heparinum* as well as its recombinant expression in *E. coli* as a highly active enzyme. We also report a biochemical characterization of its substrate specificity. Such a description provides important insight into possible structure−function relationships underlying its unusual catalytic function. It also demonstrates that the Δ4,5 glycuronidase, like the other GAG-degrading enzymes we have cloned (*20*, *28*), cleaves oligosaccharides in a nonrandom fashion. For this reason, we feel that the Δ4,5 glycuronidase is useful as a complementary enzymatic tool in our PEN-MALDI method for sequencing complex polysaccharides (*13*).

Our attempts to recombinantly express the intact glycuronidase in *E. coli* as a soluble, active protein were unsuccessful. Several attempts to refold the protein from bacterial inclusion bodies also failed. The most likely explanation for this insolubility points to the presence of a very hydrophobic region within the wild-type protein sequence spanning the first 20 amino acids. This N-terminal sequence is also predicted to comprise a cleavable prokaryotic signal sequence with the most likely cleavage site occurring between positions G20 and M21 (Figure 3). Within this sequence, we also find the alanine repeat **A**XX**A**XX-**A**XXXX**A** that may serve as part of the actual cleavage recognition sequence (*24*). This signal peptide would indicate a periplasmic location for the glycuronidase with the N-terminus of the secreted (mature) protein beginning with M21. We recombinantly expressed this mature variant ($\Delta 4,5^{\Delta 20}$) in which the signal sequence was replaced entirely by an N-terminal 6× His purification tag.

Even in our initial purifications, it was evident that our cloned Δ4,5 glycuronidase possessed a specific activity that far exceeded the activity rates reported for the flavobacterial enzyme in the early literature (*18*). These early studies, however, used only partially purified enzyme under much different reaction conditions that included milligram quanti-

ties of both substrate and enzyme. In a direct and more rigorous comparison between the recombinant and native enzymes, we find that the recombinant enzyme ($\Delta4,5^{\Delta20}$) possessed a roughly 2-fold higher specific activity relative to the native flavobacterial enzyme when measured under identical reaction conditions. From these results, it is clear that the activity of cloned enzyme is not compromised whatsoever by its recombinant expression in *E. coli*. Rather, the observed rate discrepancy is likely due to subtle differences in protein purification and storage and not to any intrinsic enzymatic properties.

The recombinant Δ4,5 glycuronidase exhibits a sharp ionic strength dependence as indicated by the shape of the NaCl titration curve (Figure 6A). These results are interesting, given both the ionic character of the disulfated heparin disaccharide used in this experiment and the many ionic residues present within the enzyme that may function in substrate binding and/or catalysis; many of these charged residues are conserved in structurally and functionally related enzymes (Figure 4). From a substrate perspective, all of the unsaturated disaccharides examined possess a negative charge (at pH 6.4) due to the C6 carboxylate of the uronic acid. It is possible that this acid acts as a critical structural determinant, especially given its proximity to the Δ4,5 bond. Charge neutralization of 6-*O*-sulfate (e.g., in $\Delta UH_{NS,6S}$) could possibly be another contributing factor. From the enzyme perspective, the recombinant glycuronidase ($\Delta4,5^{\Delta20}$) does possess 47 basic residues (theoretical p*I* of 8.5), including R151, R211, and R246 whose positions are invariantly conserved among the different glycuronidases examined. These basic amino acids may possibly interact with the uronic acid carboxylate. At the same time, Δ4,5 also possesses 44 acidic residues. At least 10 of these positions are highly conserved. Charge masking of some of these ionic residues (either acidic or basic) by increasing salt concentration might interfere with enzymatic activity. A similar observation of this ionic strength dependency has been made for the heparinases (*29*).

We also observed a bell-shaped pH profile with a 6.4 optimum. The 6.4 pH optimum generally agrees with results originally reported for the *F. heparinum* Δ4,5 as well as for more recent results published for an unsaturated glucuronyl hydrolase purified from *Bacillus* sp. GL1 (*26*). This result logically implicates one or more histidine residues functioning in catalysis. While there are 11 histidines present within the primary sequence, only three histidines (H115, H201, and H218) appear to be highly conserved. The precise catalytic function of these histidines remains to be determined. Interestingly, catalytically critical histidines also exist in all three heparin lyases (*30*) as well as chondroitin AC lyase (*31*) from *F. heparinum*. While these latter two classes of enzymes cleave glycosaminoglycans by a somewhat different mechanism compared with the Δ4,5 glycuronidase (i.e., *β*-elimination vs hydrolysis), all three enzymes would presumably involve acid−base catalysis, viz., the imidazole ring of the histidine.

We approached the question of substrate specificity from three structural perspectives: (1) the nature of the glycosidic linkage; (2) the relative sulfation pattern of the unsaturated disaccharide; and (3) the role of saccharide chain length (e.g., di- vs tetrasaccharide). As expected, our results indicate that, for the recombinant Δ4,5 glycuronidase, there is an unambiguous preference for the 1→4 linkage over the 1→3 linkage, making heparin/heparan sulfate rather than chondroitin/dermatan and/or hyaluronan the best substrate. This observation agrees with earlier, published reports (*23*) likewise indicating the critical importance of the 1→4 linkage position. It also clearly distinguishes this particular flavobacterial unsaturated glycuronidase from the chondroitin glycuronidase isolated from the same bacterium; the latter enzyme has been shown to cleave only 1→3 linked disaccharides (*32*). It should be noted, however, that while this linkage position is clearly important for heparin/heparan sulfate Δ4,5 glycuronidase substrate discrimination, it is not absolute. Both chondroitin and hyaluronan Δ4,5 disaccharides were hydrolyzed, albeit at much slower rates and using higher enzyme concentrations than were required to hydrolyze heparin disaccharides.

We also present a kinetic pattern of the Δ4,5 glycuronidase with regard to the specific sulfation within a heparin disaccharide. First and foremost, we find that unsaturated saccharides containing a 2-O-sulfated uronidate (ΔU_{2S}) at the nonreducing end are uncleavable by the Δ4,5 glycuronidase. Furthermore, the inability of a 2-O-sulfated disaccharide to competitively inhibit the hydrolysis of non-2-O-containing disaccharide substrates (such as ΔUH_{NAc}) further suggests that the presence of a 2-*O*-sulfate precludes binding of this saccharide to the enzyme (data not shown). Therefore, 2-O-sulfation, along with linkage position, is another unequivocal structural constraint. On the basis of these observations, it is also clear that, both in vivo and in vitro, the 2-O-position of the unsaturated uronidate must first be desulfated if the Δ4,5 glycuronidase is to subsequently hydrolyze the glycosidic bond.

In considering the effect of specific sulfate groups present on the glucosamine, the enzyme may be loosely summarized as having a graded preference for 6-O-sulfation but a clear selection against unsubstituted or sulfated amines. We must emphasize that this hierarchy is not an absolute distinction given the fact that the enzyme cleaved all the non-2-O-containing heparin disaccharides that we examined. Instead, it is based on relative kinetic parameters (Table 2). This apparent substrate discrimination at the N-and 6-positions of the glucosamine appears to be somewhat contextual, especially in the case of 6-O-sulfation. That is, while 6-O-sulfation may bestow a favorable selectivity to a saccharide substrate, this positive effect is offset by the presence of a deacetylated amine (e.g., $\Delta UH_{\mathbf{NAc},6S}$ vs $\Delta UH_{\mathbf{NH2},6S}$ or $\Delta UH_{NS,6S}$). While the exact reason for this structural discrimination needs to be investigated, it is tempting to speculate a positive role of the acetate itself, e.g., in satisfying an important van der Waals interaction.

We feel that the unequivocal bias the Δ4,5 demonstrates against 2-O-sulfated uronidates along with a so-called "N-position" discrimination for the glucosamine can be exploited for use of the glycuronidase as an analytical tool for the compositional analyses of heparinase-treated oligosaccharides. In fact, we were able to predict the extent and relative rates by which specific disaccharide species would disappear (i.e., due to the glycuronidase-dependent loss of absorbance at 232 nm), based entirely on our kinetically defined substrate specificity determinations (Figure 8). As expected, all 2-*O*-sulfate-containing disaccharides were refractory to hydrolysis by the Δ4,5 glycuronidase. On the other hand, the remaining

disaccharides were hydrolyzed in a time-dependent fashion that corresponded to their relative substrate specificities (i.e., $\Delta UH_{NAc,6S} > \Delta UH_{NS,6S} > \Delta UH_{NS}$).

From this experiment, another important observation was made, namely, that the Δ4,5 glycuronidase also hydrolyzes Δ4,5 unsaturated tetrasaccharides. It is also very interesting to note that this particular tetrasaccharide is as good a substrate as the disaccharide ΔUH_{NS}. This observation may argue against a substrate discrimination used by the enzyme that is negatively based on increasing molecular mass (at least up to a tetrasaccharide) as was first reported (*23*). It also leaves open the possibility that the Δ4,5 glycuronidase interacts predominantly with the unsaturated disaccharide unit residing at the nonreducing end. The actual effect of oligosaccharide chain length on relative glycuronidase activity has to be more thoroughly examined. In particular, it will be useful to address structure−activity relationships as they pertain to internal saccharide positions.

The Δ4,5 unsaturated glycuronidase is an interesting and unusual enzyme whose catalytic mechanism merits further investigation. The work presented here is foundational to future studies relating molecular structure to this function. At the same time, its unique substrate specificity makes this enzyme an excellent tool for characterizing HSGAG composition and fine structure.

ACKNOWLEDGMENT

We thank Kevin Pojasek for a critical reading of the manuscript and for helpful suggestions. We also thank Joseph Davis for technical assistance.

REFERENCES

1. Habuchi, O. (2000) *Biochim. Biophys. Acta 1474*, 115−127.
2. Tumova, S., Woods, A., and Couchman, J. R. (2000) *Int. J. Biochem. Cell Biol. 32*, 269−288.
3. Folkman, J., Taylor, S., and Spillberg, C. (1983) *Ciba Found. Symp. 100*, 132−149.
4. Blackhall, F. H., Merry, C. L., Davies, E. J., and Jayson, G. C. (2001) *Br. J. Cancer 85*, 1094−1098.
5. Shukla, D., Liu, J., Blaiklock, P., Shworak, N. W., Bai, X., Esko, J. D., Cohen, G. H., Eisenberg, R. J., Rosenberg, R. D., and Spear, P. G. (1999) *Cell 99*, 13−22.
6. Perrimon, N., and Bernfield, M. (2000) *Nature 404*, 725−728.
7. Lyon, M., Rushton, G., Askari, J. A., Humphries, M. J., and Gallagher, J. T. (2000) *J. Biol. Chem. 275*, 4599−4606.
8. Esko, J. D., and Lindahl, U. (2001) *J. Clin. Invest. 108*, 169−173.
9. Conrad, H. (1998) *Heparin-binding proteins*, Academic Press, New York.
10. Drummond, K. J., Yates, E. A., and Turnbull, J. E. (2001) *Electrophoresis 22*, 304−310.
11. Calabro, A., Midura, R., Wang, A., West, L., Plaas, A., and Hascall, V. C. (2001) *Osteoarthritis Cartilage 9*, S16−S22.
12. Rhomberg, A. J., Ernst, S., Sasisekharan, R., and Biemann, K. (1998) *Proc. Natl. Acad. Sci. U.S.A. 95*, 4176−4181.
13. Venkataraman, G., Shriver, Z., Raman, R., and Sasisekharan, R. (1999) *Science 286*, 537−542.
14. Shriver, Z., Raman, R., Venkataraman, G., Drummond, K., Turnbull, J., Toida, T., Linhardt, R., Biemann, K., and Sasisekharan, R. (2000) *Proc. Natl. Acad. Sci. U.S.A. 97*, 10359−10364.
15. Payza, A. N., and K., E. D. (1956) *J. Biol. Chem. 223*, 853−858.
16. Linker, A., and Hovingh, P. (1965) *J. Biol. Chem. 240*, 3724−3728.
17. Dietrich, C. P. (1969) *Biochem. J. 111*, 91−95.
18. Warnick, C. T., and Linker, A. (1972) *Biochemistry 11*, 568−572.
19. McLean, M. W., Bruce, J. S., Long, W. F., and Williamson, F. B. (1984) *Eur. J. Biochem. 145*, 607−615.
20. Sasisekharan, R., Bulmer, M., Moremen, K. W., Cooney, C. L., and Langer, R. (1993) *Proc. Natl. Acad. Sci. U.S.A. 90*, 3660−3664.
21. *Current Protocols in Molecular Biology* (1987), John Wiley and Sons, New York.
22. Nielsen, H., Engelbrecht, J., Brunak, S., and von Heijne, G. (1997) *Protein Eng. 10*, 1−6.
23. Hovingh, P., and Linker, A. (1977) *Biochem. J. 165*, 287−293.
24. von Heijne, G. (1988) *Biochim. Biophys. Acta 947*, 307−333.
25. Linker, A. (1979) *Biochem. J. 183*, 711−720.
26. Hashimoto, W., Kobayashi, E., Nankai, H., Sato, N., Miya, T., Kawai, S., and Murata, K. (1999) *Arch. Biochem. Biophys. 368*, 367−374.
27. Linker, A., Hoffman, P., Meyer, K., Sampson, P., and Korn, E. D. (1960) *J. Biol. Chem. 235*, 3061−3065.
28. Pojasek, K., Shriver, Z., Kiley, P., Venkataraman, G., and Sasisekharan, R. (2001) *Biochem. Biophys. Res. Commun. 286*, 343−351.
29. Lohse, D. L., and Linhardt, R. J. (1992) *J. Biol. Chem. 267*, 24347−24355.
30. Pojasek, K., Shriver, Z., Hu, Y., and Sasisekharan, R. (2000) *Biochemistry 39*, 4012−4019.
31. Huang, W., Boju, L., Tkalec, L., Su, H., Yang, H. O., Gunay, N. S., Linhardt, R. J., Kim, Y. S., Matte, A., and Cygler, M. (2001) *Biochemistry 40*, 2359−2372.
32. Gu, K., Linhardt, R. J., Laliberte, M., and Zimmermann, J. (1995) *Biochem. J. 312*, 569−577.

BI012147O